Energy Management for Fuel Cell/Battery Hybrid Unmanned Aerial Vehicle

Zhibo Cheng, Huiying Liu, Peiran Yu, Lin Zhu, Tianhao Sun, Yongming Yao[*]

School of Mechanical and Aerospace Engineering, Jilin University, 130025 Changchun, China
[*]E-mail: ymyao@jlu.edu.cn

The poor endurance of battery-powered unmanned aerial vehicles (UAVs) can be improved by applying a fuel cell hybrid system. Energy management can significantly affect the hybrid system performance. Energy management in fuel cell/battery hybrid fixed-wing UAVs is challenged by the variable flight conditions of the UAVs and the complex energy flows in the hybrid system. This study first establishes a mathematical model of the fuel cell/battery hybrid fixed-wing UAV. Next, four energy management strategies (EMSs), namely fuzzy logic, dynamic programming, Pontryagin's minimum principle (PMP), and improved PMP, are proposed. The improved PMP-based EMS considers the fuel cell current and the power changing rate. The simulation results based on the actual working load of a fixed-wing UAV in the MATLAB environment show that the proposed EMSs are effective in extending the UAV endurance while reducing the change rate of the fuel cell output power and improving adverse effects on the battery lifetime. The methodologies presented herein can be applied to other UAVs and hybrid systems.

1. INTRODUCTION

In the context of the growing demand for unmanned aerial vehicles (UAVs) in military and civilian applications [1], researchers are placing higher demands on the UAV power system performance. UAVs powered by internal combustion engines with high power and energy densities have a satisfactory power performance, but also have the disadvantages of low efficiency [2] and obvious acoustic and thermal characteristics [3]. Meanwhile, running internal combustion engines consumes fossil fuel, such as gasoline and diesel fuel, while inevitably emitting greenhouse gases into the atmosphere. Along with the fossil fuel depletion and the growing importance of environmental protection, the use of environmentally friendly energy sources such as electric power to replace internal combustion engines in UAVs is imminent.

Despite the advantages of electric-powered UAVs with low thermal characteristics and no polluting gas emissions [4], most of the UAVs currently designed and manufactured by the world's major UAV manufacturers, such as DJI-innovations and Parrot, only use batteries to provide the energy needed for flight. The power performance of these UAVs is limited by the battery performance. A lithium-ion battery typically has a specific energy of 120–240 Wh/kg and a specific power of 1000–3000 W/kg and can be discharged for 10–60 min [5]. The flight time and the durability of UAVs with batteries as the sole power source are limited by the poor battery performance. Improving the range of UAVs can be started by applying a power source with a greater energy density compared to batteries to the UAVs.

Applying fuel cells in UAVs is a promising method to extend the range. As a different power source from batteries, fuel cells have the characteristics of high system efficiency, zero-emission characteristics [6], and ideal power density. Some scholars estimate that with the development of the hydrogen storage technology, the energy density of fuel cells can reach 1000 Wh/kg [7], which is far greater than the battery and can effectively improve the range of the power system. Taking HYCOPTER drones with fuel cells as the main power source, for example, such UAVs can achieve a maximum range of approximately 3.5 h by adjusting the size of the energy storage unit and the payload weight, to be much longer than battery-powered UAVs. However, applying fuel cells to UAV power systems faces the challenges of poor dynamic response and low power density [8], which affect the maneuverability of UAVs and make fuel cells unsuitable for supplying energy to UAVs in situations where the UAV power demand changes drastically. In addition, fuel cells cannot absorb and regenerate energy.

The weaknesses of the fuel cell can be compensated for by forming a hybrid power source through mixing fuel cells with other power sources [9]. The power system of a hybrid UAV should have two components: a fuel cell used to provide most of the UAV's energy requirements and an auxiliary energy source that can both store electrical energy and release energy. Auxiliary power sources include batteries, supercapacitors, a combination of both, etc. By combining fuel cells with batteries, a power source with a better dynamic performance can be realized, and the lack of a dynamic response performance of fuel cells can be compensated for to form a hybrid system.

The energy management strategy (EMS) reasonably decides on the power distribution among multiple power sources according to the different characteristics of multiple components and the power requirements of different UAV flight phases, thus improving the system efficiency, energy saving, or other performance. For a hybrid system consisting of a fuel cell and a battery, the output performance of the hybrid power system affects the fuel cell lifetime [10]. An ideal control strategy can extend the battery life while reducing the hydrogen consumption [11]. The control strategies currently applied in hybrid power systems can be summarized into two main categories: rule- and optimization-based strategies. The rule-based strategy operates the power system in different modes through pre-designed control rules and compares the parameters of the hybrid power system operation with predefined parameters. Typical rule-based strategies, such as the state machine strategy [12–14] and the fuzzy logic [15], have the advantage of low computational cost and is easy to realize online. The disadvantage of this type of strategy is that the set of rules and parameters depends on the designer's knowledge of the load power and different power supply characteristics. Optimization-based strategies achieve energy management by minimizing predefined objective functions. All of them can be further divided into two parts: global optimization- and transient optimization-based strategies. Dynamic programming (DP)

[16], Pontryagin's minimum principle (PMP) [17], and genetic algorithm (GA) [18] are three typical global optimization algorithms, that bear a large computational burden and are usually used to control the energy allocation for a specific cycle. Their results can be used as benchmarks to measure the advantages and disadvantages of other algorithms in energy management. The equivalent consumption minimization strategy (ECMS) [19,20] and the model predictive control (MPC) [21] are transient optimization-based energy management methods. Although these algorithms cannot guarantee global optimality, they have the obvious advantages of being independent of specific operating cycles, relatively small computational effort, and ease of implementation.

Multiple methods can be combined or new algorithms can be used to increase the effectiveness of energy management. Xie et al. [22] proposed a stochastic model predictive controller. The strategy was more computationally efficient than DP–MPC, did not require a dynamic adjustment of the equivalence factor compared to the ECMS–MPC, and achieved a near-global optimal performance with a faster computation. Marzougui et al. [23] proposed an EMS combining three strategies of state machine strategy, flatness control, and fuzzy logic for a hybrid system. This strategy can regulate the out power of the fuel cell by fuzzy logic control when the operating conditions are unknown and allocate the power flow of the battery by relying on a rule-based strategy while allocating the output power of the supercapacitor by flatness control. Bassam et al. [24] proposed a multiprogram EMS for reducing the energy consumption of a hybrid powertrain. The strategy was pre-designed with four EMSs, namely state machine strategy, ECMS, CDCS, and classical PI. The strategy allowed the system to switch operations between the four different strategies based on the current situation. The proposed multiprogram EMS was more energy saving compared to the four strategies operating individually. Zhang et al. [25] proposed a simulation platform that combined the UAV model with a hybrid power system model and designed a fuzzy state machine-based EMS for it with online application potential. The control strategy combines the state machine strategy with fuzzy logic to distribute the power flow among three different power elements. The performed simulations demonstrated that this strategy saves 26.7% of hydrogen fuel compared to the thermostat control strategy, thereby providing better fuel economy. Rezk et al. [26] proposed two new energy management methods, called the salp swarm and mine explosion algorithms, and conducted a comparative study of nine different strategies. The salp swarm algorithm-based external energy maximization strategy showed the highest system efficiency and the lowest hydrogen consumption.

The present study investigates the design and analysis of a hybrid power system for UAV applications. We hope to solve the durability problem of the hybrid system and obtain an attractive performance using some control strategies. The remainder of this paper is organized as follows: Section 2 presents an analysis of the electrical system topology for a hybrid UAV, including the energy flow analysis of the hybrid system; Section 3 introduces the four proposed control strategies, namely fuzzy logic, basic PMP, improved PMP, and DP; Section 4 discusses the simulation of the four proposed strategies; and Section 5 provides the conclusions of this study.

2. SYSTEM DESCRIPTION AND SYSTEM MODEL

The hybrid UAV topology is analyzed in this section. The energy flows are considered, and the model of a hybrid-powered UAV is established.

2.1 System description and energy flow analysis

Fixed-wing UAVs are usually composed of several components, including fuselage, wings, energy storage system, and powertrain system. The lift and the attitude torque required for the UAV flight are provided by the wing, which can be further divided into main wings, aileron wings, etc. Figure 1 shows the main components of the proposed UAV hybrid system, which are different from those of a traditional UAV power system. The unidirectional DC/DC converter has the function of matching voltage. The bidirectional DC/DC is used to adjust the working current of the battery.
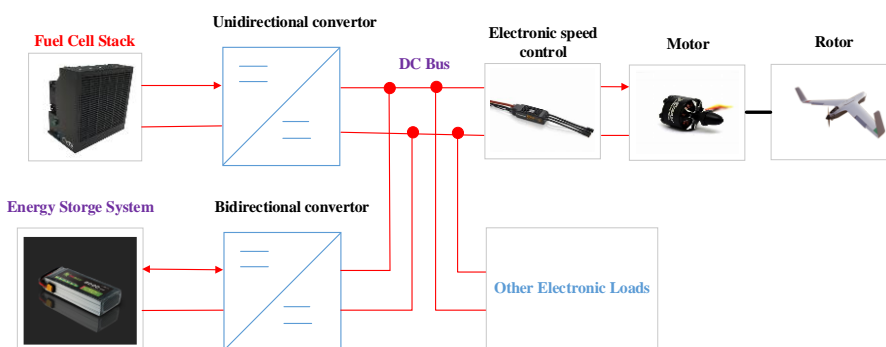

Figure 1. Topology of the hybrid UAV.

Figure 2 illustrates the energy flows in the hybrid-powered UAVs. Two different energy sources worked simultaneously in a hybrid-powered system to meet the different power requirements of the UAV in performing complex missions, whether it is a flat power demand or a drastically changing power demand. The fuel cell stack was installed to a boost DC/DC converter, while the battery was installed to a bidirectional DC/DC converter that allowed the current to flow in both directions. As the main energy source, the changes in the output power of the fuel cell should be limited. The additional energy required by the UAV during a sudden increase in the power demand should mainly be provided by the battery, which can also act as an energy storage element to absorb the excess energy released by the fuel cell. The energy management system regulates the duty cycle of each DC/DC converter by receiving information, such as load power and battery state of charge (SoC), to control the power of different power supplies, such that each energy supply operates in the ideal operating state.
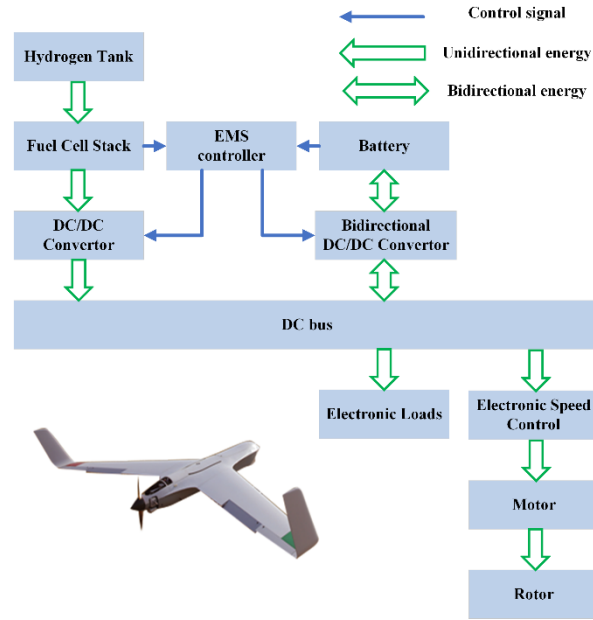
Figure 2. Energy flows in the hybrid UAV.

2.2 Fuel cell model

The fuel cell is an electrochemical element with many classifications. Among the many types of fuel cells, the polymer electrolyte membrane fuel cell (PEMFC) is believed to be the most promising option for UAV applications [27]. The output voltage of the PEMFC is calculated as follows [28]:

$$V_{cell} = E_{Nernst} - V_{act} - V_o - V_{con} \tag{1}$$

$$E_{Nernst} = 1.299 - (8.5 \times 10^{-4})(T - 298.15) + 4.308 \times 10^{-5} \times T \times ln(P_{H_2}^* + \frac{1}{2}P_{O_2}^*) \tag{2}$$

$$V_{act} = \xi_1 + \xi_2 \cdot T + \xi_3 \cdot T \cdot ln(I_{fc}) + \xi_4 \cdot T \cdot ln(C_{O_2}^*) \tag{3}$$

$$C_{O_2}^* = P_{O_2}/[5.08 \times 10^{-6} exp(-498/T)] \tag{4}$$

$$V_o = I_{fc} \cdot R_o = I_{fc} \cdot (R_{membrane} + R_{contact}) \tag{5}$$

$$R_{membrane} = \frac{r_m \cdot t_m}{A_m} \tag{6}$$

$$V_{con} = B(1 - \frac{J}{J_{max}}) \tag{7}$$

where, E_{Nernst} is the Nernst potential; V_{act} is the overvoltage caused by activation; V_o is the overvoltage caused by ohmic loss; V_{con} is the overvoltage caused by concentration losses; T is the operating temperature of the fuel cell; $P_{H_2}^*$ is the effective pressure of hydrogen gas; $P_{O_2}^*$ is the effective pressure of oxygen; ξ_i is a parameter measured by the experiment; $C_{O_2}^*$ is the oxygen concentration in the liquid phase of the anode; P_{O_2} is the partial pressure of oxygen at the cathode; I_{fc} is the fuel cell operating current; t_m is the proton exchange membrane thickness, A_m is the effective area of the proton exchange membrane; r_m is the resistivity of the proton exchange membrane related to the actual operating state of the fuel cell; B is a constant determined by the fuel cell and operating state; and J is the current density.

The overvoltage caused by the fuel cell activation reflects the energy consumed to move the electrons from the cathode to the anode [29]. The overvoltage caused by the ohmic loss of a fuel cell comprises the voltage drop caused by both the equivalent membrane impedance $R_{membrane}$ and the

contact impedance between the membrane and the electrode plate $R_{contact}$, which describes the impedance of the conductor to the charge when the charge flows in the conductor. Meanwhile, the overvoltage caused by the concentration loss reflects the voltage drop caused by an untimely supply of hydrogen and oxygen when the fuel cell current density is too high. Figure 3 shows the output characteristics of the fuel cell stack (FCS). The PEMFC consumes hydrogen at different rates at different power outputs, which can be expressed as follows [30]:

$$C_{fc} = N \cdot \frac{M_{H_2}}{n_e \cdot F} \cdot I_{fc} \tag{8}$$

where, N is the number of cells; M_{H_2} is the molar mass of hydrogen; n_e is the number of electrons; and F is Faraday's constant.
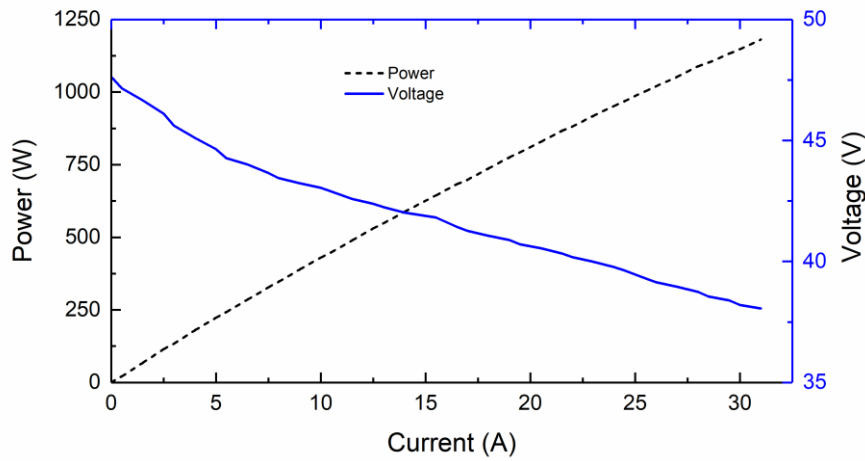

Figure 3. Characteristics of a 1000W PEMFC.

2.3 Battery model

A plausible battery model is critical to the study of hybrid system EMSs. We used the PNGV equivalent circuit model to depict the battery characteristics and the operating current. Figure 4 depicts the battery equivalent circuit model.

$$I_{bat} = \{U_{ocv} - U_p - \left[\left(U_{ocv} - U_p \right)^2 - 4 * R_o * P_{bat} \right]^{\frac{1}{2}} \}/2 * R_o \tag{9}$$

where, I_{bat} is the operating current; U_{ocv} is the open-circuit voltage; U_p denotes the polarization effect parameters of the cell; and R_o is the internal resistance. The SoC can be calculated in real time using the Coulomb counting method.

$$SoC(k+1) = SoC(k) - \frac{\eta * I_{bat}(k)}{Q_{max}} \cdot \Delta t \tag{10}$$

$$V_{cell} = E_{cell} - V_{act} - V_{ohm} \tag{11}$$

where, η denotes the charging and discharging efficiency of the battery, and Q_{max} denotes the maximum battery capacity.
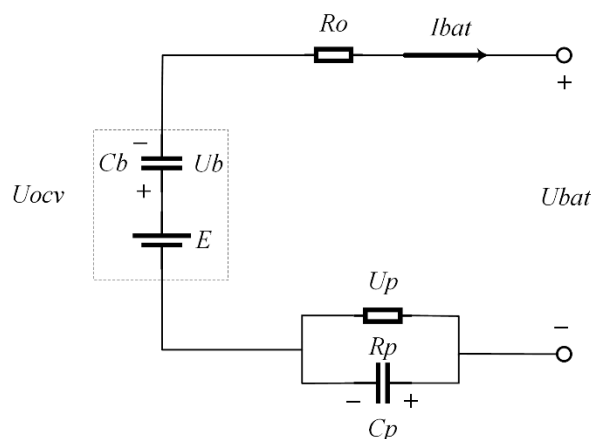
Figure 4. Battery equivalent circuit model.

2.4 DC/DC model

In the hybrid-electric propulsion system proposed herein, the fuel cell system and the battery system were installed to the DC bus using two DC/DC converters for precisely control the working conditions of the fuel cells and the batteries. Considering the fast response of the DC/DC converters, the power relationship between the input and the output of the DC/DC converters is described by the efficiency with power loss. The relationship between the power at the input and that in the output of the DC/DC converters is calculated as follows:

$$P_{out}(t) = P_{in}(t) \cdot \eta_i - P_{loss}(t) \tag{12}$$
$$P_{in} = U_{in} \cdot I_{in} \tag{13}$$
$$P_{out} = U_{out} \cdot I_{out} \tag{14}$$

where, P_{out} is the output power of the DC/DC converters; P_{in} is the input power of the DC/DC converters; η is the DC/DC converter efficiency; P_{loss} is the power loss in the DC/DC converters; U_{in} and I_{in} are the input voltage and the current, respectively; and U_{out} and I_{out} are the output voltage and current, respectively.

2.5 Fixed-wing UAV powertrain model

The powertrain of a fixed-wing UAV mainly includes three parts: motor, electronic speed control, and propeller. The powertrain is an important component of the fuel cell hybrid UAV, which receives energy from the energy storage system and converts this energy from electrical into mechanical energy to provide the torque needed for the UAV.

$$P_{dem}(t) = P_M(t) \cdot \eta_M(t) \tag{15}$$
$$P_M(t) = T_M(t) \cdot \omega_M(t) \tag{16}$$

where, P_{dem} is the demand power of UAV; P_M is the motor power; η_M is the motor efficiency; T_M is the motor torque; and ω_M is the motor speed.

The efficiency of the electronic speed control and the motor is relatively constant during the UAV flight. We assume that the efficiency of the electronic speed control is constant at 90% , while that of the motor is constant at 80%. The motor model is [25].

$$M_m = (I_m - I_0) \cdot \frac{30}{\pi \cdot k_V} \qquad (17)$$

$$I_m = \frac{U_m - \Omega/k_v}{r_m} \qquad (18)$$

where, M_m is the motor torque; I_m is the motor current; I_0 is the current when the motor has no load; k_V is the speed constant of the motor; U_m is the terminal voltage of the motor; r_m is the motor terminal resistance.

The pull and torque generated by the propeller are calculated as follows:

$$M = \frac{4}{\pi^3} \cdot \rho \cdot R^5 \cdot \omega^2 \cdot C_Q \qquad (19)$$

$$T = \frac{4}{\pi^2} \cdot \rho \cdot R^4 \cdot \omega^2 \cdot C_T \qquad (20)$$

where, M is the torque generated by the propeller; R is the radius of the propeller; ω is the propeller speed; C_Q is the torque factor of the propeller; and C_T is the pull factor of the propeller.

3. ENERGY MANAGEMENT STRATEGY DEVELOPMENT

Energy management must achieve various purposes, including the reduction of the system hydrogen consumption, improvement of the system efficiency, and enhancement of the power source durability to achieve a reasonable power distribution among different power sources. The energy balance equation of the UAV bus is calculated as:

$$P_{bus}(t) = P_{ref}(t) + P_{aux}(t) \qquad (21)$$

$$P_{bus}(t) = P_{fc}(t) * \eta_{DC1} + P_b(t) * \eta_{DC2} \qquad (22)$$

where, P_{bus} is the DC bus power for the UAV; P_{ref} is the reference power for the UAV; and η_{DC1} and η_{DC2} are the energy conversion efficiency of the unidirectional DC/DC and bidirectional DC/DC converters, respectively.

3.1 Fuzzy logic-based EMS

The proposed fuzzy logic controller has two input variables and one output variable. The input variables are the power required for the UAV flight P_{ref} and the battery SoC. The output variable is the fuel cell output power P_{fc}. The demand power is divided into five states denoted by very low (VL), low (L), middle (M), high (H), and very high (VH).
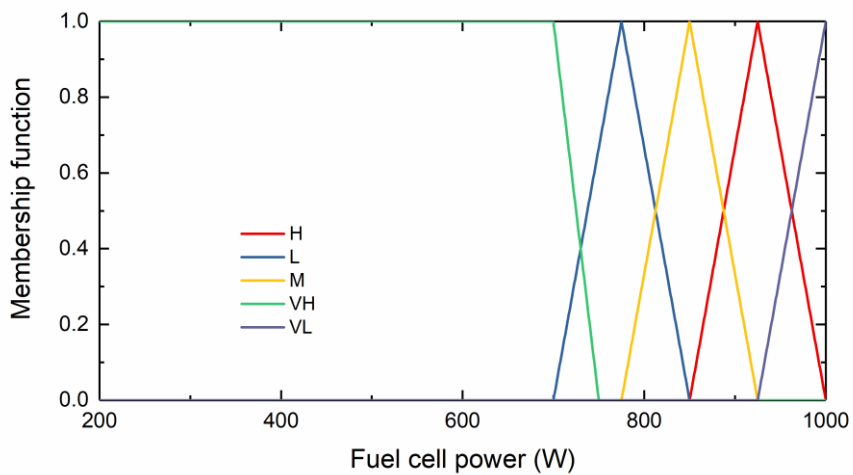
Table 1. Fuzzy logic rules

P_{fc}		P_{ref}				
		VL	L	M	H	VH
SoC	H	VL	VL	VL	L	M
	M	VL	VL	L	H	H
	L	L	L	M	H	H
	VL	M	M	H	VH	VH
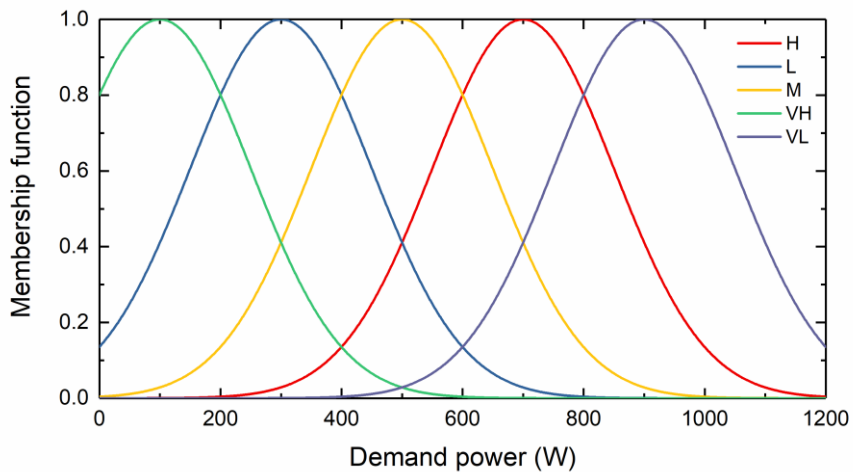
(a)
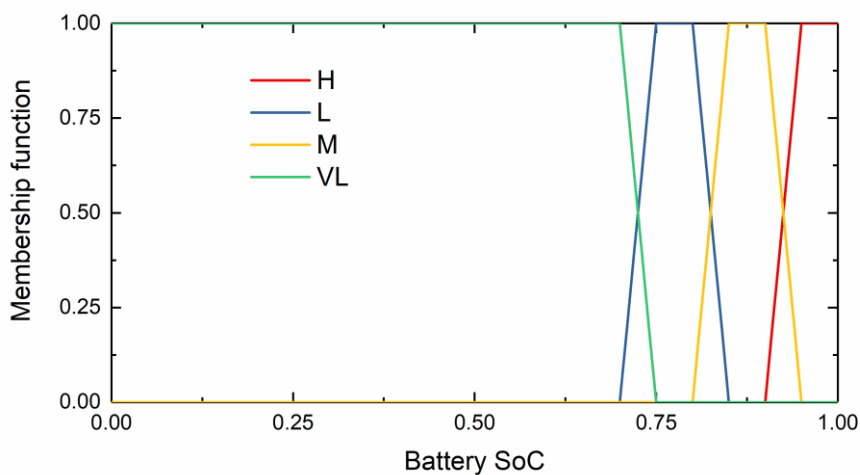
(b)

(c)

Figure 5. Membership functions of the fuzzy logic controller. (a): Demand power; (b): Battery SoC; (a): Fuel cell power.

The battery SoC was categorized into four states denoted as very low (VL), low (L), middle (M), and high (H). P_{fc} was divided into five states: very low (VL), low (L), middle (M), high (H), and very high (VH). Table 1 presents the rule base of the fuzzy rules, which include 20 rules. Figure 5 shows the membership functions of P_{fc}, SoC, and P_{ref}. Mamdani's fuzzy inference approach was used along with the centroid method for defuzzification.

3.2 PMP-based EMS

As a theory of optimal control, PMP transforms the global optimization problem into a series of minimal value problems and obtains a sequence of optimal solutions by solving one minimal value problem at each instant. By adding cost functions or state variables, researchers can use the PMP to reduce the hydrogen consumption or improve the service life of fuel cells and batteries. The PMP aims to find the optimal trajectory of the control variable P_{fc} that can reduce the hydrogen consumption, control the degree of change in the fuel cell power, and maintain the battery SoC within a reasonable range. A fuel cell/battery hybrid UAV has only one state variable in the system. The equation of state can be calculated as follows:

$$\dot{SoC}(t) = g(SoC(t), P_{fc}(t), t) \qquad (23)$$

$$\dot{SoC} = -\frac{I_b}{Q_{max}} = -\{\frac{U_{ocv} - U_p - \left[(U_{ocv} - U_p)^2 - 4*R_o*P_L\right]^{\frac{1}{2}}/2*R_o}{Q_{max}}\} \qquad (24)$$

where, the state variable $\dot{SoC}(t)$ is a function of $SoC(t)$, $P_{fc}(t)$ and t.

The excessive depth of the battery discharge will damage the battery's durability. The battery SoC must be kept within a reasonable range. When studying the basic PMP, the cost function L_1 is defined to impose constraints on the battery SoC and extend the battery durability, as below:

$$L_1\left(P_{fc}(k)\right) = \begin{cases} \alpha_1 \cdot P_{fc}(k), & SoC(k) < SoC_{VL} \\ \alpha_2 \cdot P_{fc}(k), & SoC_{VL} < SoC(k) < SoC_L \\ 0, & SoC_L < SoC(k) < SoC_H \\ \alpha_3 \cdot P_{fc}(k), & SoC_H < SoC(k) < SoC_{VH} \\ \alpha_4 \cdot P_{fc}(k), & SoC(k) > SoC_{VH} \end{cases} \qquad (25)$$

where, α_1, α_2, α_3, and α_4 are constant tuning parameters, and k is the time step.

During the actual UAV flight, the actual power demand dramatically changes, which can easily cause a drastic change in the fuel cell. Dramatic changes have adverse effects on the fuel cell durability. Therefore, one must consider limiting the change rate of the fuel cell power. In hybrid UAVs, more attention should be paid to the durability of the FCS. The changes in the fuel cell power must be restricted. When the power demand fluctuates, the EMS should control the battery to cope with the fluctuation while keeping the fuel cell output power relatively stable. The high current density caused by the excessive fuel cell power is also harmful to the fuel cell durability. The improved PMP constrains both the fuel cell power variation rate and the fuel cell power by L_2, as follows:

$$L_2\left(P_{fc}(k)\right) = \beta_1 \cdot P_{fc}(k) + \beta_2 \cdot \left(P_{fc}(k) - P_{fc}(k-1)\right)^2 \qquad (26)$$

where, β_1 and β_2 are tuning parameters.

The Hamiltonian function of the basic PMP is expressed in formula (27). The Hamiltonian function of the improved PMP is expressed in formula (28) based on the basic PMP.

$$H\big(\dot{SoC}(k), P_{fc}(k), k\big) = \dot{m}_{H_2}(k) + \lambda(k) \cdot \dot{SoC}(k) + L_1\big(P_{fc}(k)\big) \tag{27}$$

$$H\big(\dot{SoC}(k), P_{fc}(k), k\big) = \dot{m}_{H_2}(k) + \lambda(k) \cdot \dot{SoC}(k) + L_1\big(P_{fc}(k)\big) + L_2\big(P_{fc}(k)\big) \tag{28}$$

where, $\dot{m}_{H_2}$ is the instantaneous hydrogen consumption; and λ is the co-state variable.

The objective function of the improved PMP consists of four components. The first part is used to regulate the hydrogen consumption of the fuel cell. The second part is used to control the battery current. The third part is utilized to maintain the battery SoC within a reasonable range to avoid damage to the battery's durability due to overcharging or overdischarging. The fourth part can smooth the output power curve of the fuel cell by limiting the change of the output power while avoiding the heavy load output. The Hamiltonian used to solve the optimal control problems is presented as follows:

$$\begin{cases} \dot{SoC}^*(t) = \dfrac{\partial H}{\partial \lambda}(SoC^*(t), P_{fc}^*(t), \lambda^*(t)) \\ \dot{\lambda}^*(t) = -\dfrac{\partial H}{\partial SoC}(SoC^*(t), P_{fc}^*(t), \lambda^*(t)) \end{cases} \tag{29}$$

$$H(SoC^*(k), P_{fc}^*(k), \lambda^*(k)) \leq H(SoC^*(k), P_{fc}(k), \lambda^*(k)) \tag{30}$$

where, $*$ enotes the optimal variable values.

In the proposed hybrid system, limiting the change rate of the fuel cell output power while imposing constraints on the fuel cell power and the current is beneficial for the fuel cell endurance. This limiting of the SoC of the battery between $[SoC_{min}, SoC_{max}]$ had a positive effect on prolonging the battery life. The initial SoC of the battery was set to 0.8. These constraints are summarized as follows:

$$\begin{cases} P_{fc,min} \leq P_{fc}(k) \leq P_{fc,max} \\ 0 \leq \Delta P_{fc}(k) \leq \Delta P_{fc,max} \\ SoC_{min} \leq SoC(k) \leq SoC_{max} \\ SoC_{t_0} = 0.8 \\ 0 \leq I_{fc}(k) \leq I_{fcmax} \end{cases} \tag{31}$$

where, $P_{fc,min}$ is the minimum power output of the fuel cell; $P_{fc,max}$ is the maximum power output of the fuel cell; $\Delta P_{fc,max}$ is the maximum change rate of the fuel cell power; SoC_{min} is the minimum state of charge of the battery; SoC_{max} is the maximum state of charge of the battery; and $I_{fc,max}$ is the maximum current of the fuel cell.

3.3 DP-based EMS

The DP solves multi-stage decision problems by processing complex problems in steps. The DP application must obtain the global information of the UAV flight power in advance. Therefore, the DP is more suitable as an offline algorithm that serves as a benchmark for other strategies. The objective function yields by DP is shown below:

$$J(k) = \sum_{k=0}^{N-1} L\left(SoC(k), P_{fc}(k), k\right) \tag{32}$$

$$L\big(SoC(k), P_{fc}(k), k\big) = \dot{m}_{H_2}(k) + \gamma_1 \cdot \big(SoC(k) - SoC_{ref}\big)^2 + \gamma_2 \cdot I_{fc}(k) \tag{33}$$

where, γ_1 and γ_2 are constant paraments; and SoC_{ref} is a pre-designed value of SoC.

The objective function of the DP consists of three parts. The first part imposes constraints on the rate of hydrogen depletion in the fuel cells. The second part imposes constraints on the SoC of the battery.

The third part can avoid excessive fuel cell current. A set of constraints was established by the PMP. The initial and terminal values of the state variables should be the same during the use of the DP. Bellman's principle states that the recursive equation solving the objective function of the DP is as follows.

$$J^*_k\big(SoC(k)\big) = max\big[L\big(SoC(k), P_{fc}(k), k\big) + J^*_{k+1}\big(SoC(k+1)\big)\big] \quad k = N-1, N-2, \dots, 1, 0 \quad (34)$$

where, J^*_k is the optimal solution at the k-th moment and $J^*_N = 0$.

4. RESULTS AND DISCUSSION

In this section, the hybrid UAV will be tested in the MATLAB environment using fuzzy logic, basic PMP, improved PMP, and DP-based EMSs. Figure 6 presents the power spectrum of the test UAV from the literature [15]. This section compares the three EMS mentioned in reference [15] using the FL, PMP, improved PMP and DP algorithms. The tuning parameters in the EMSs are set as α_1=-0.02, α_2=-0.005, α_3=0.005, α_4=0.02, β_1=0.0003, β_2=0.0005, γ_1=1300, γ_2=0.5. Figures 7–10 show the simulation results of the four strategies for the UAV flight cycle in terms of the fuel cell power, battery power, battery SoC, and change rate of the FCS net power. The simulation results from Figures 7–9 illustrate that the hybrid system based on the proposed strategy can achieve reasonable power splitting under load variation. Figure 8 depicts that the battery can both absorb electrical energy from the fuel cell when the UAV demand power is low and release electrical energy when the UAV is flying under heavy loads. Figure 10 demonstrates that the proposed EMS can effectively reduce the fuel cell power fluctuation in the hybrid system, control the fuel cell operation, and have a protective effect on the FCS life.
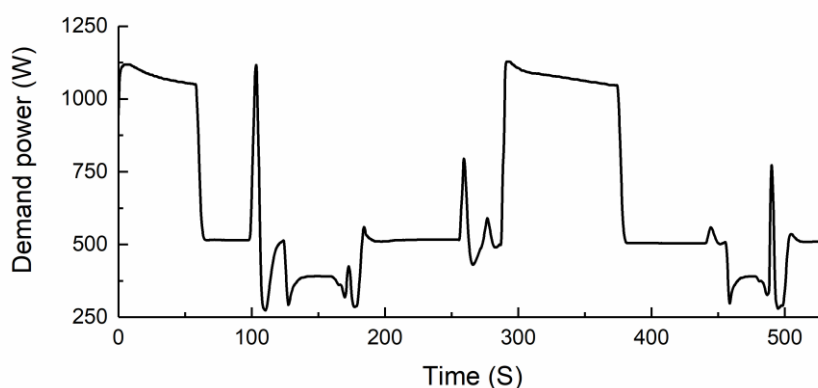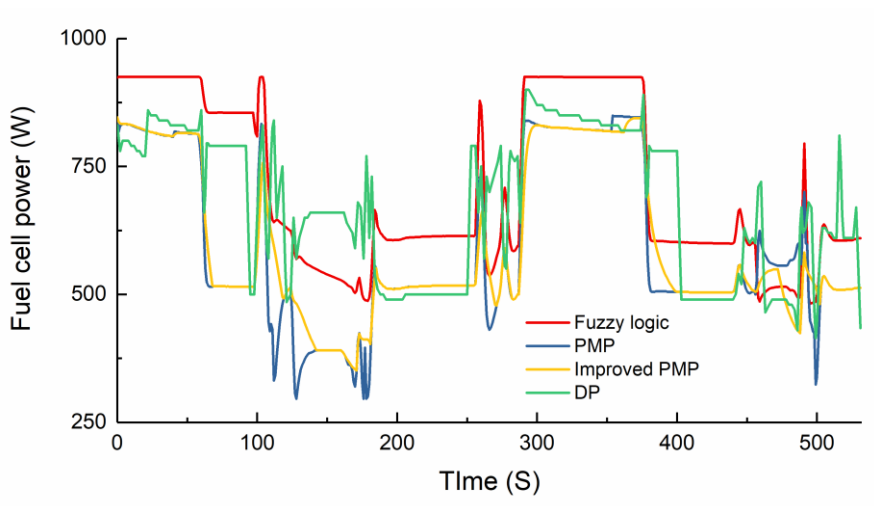

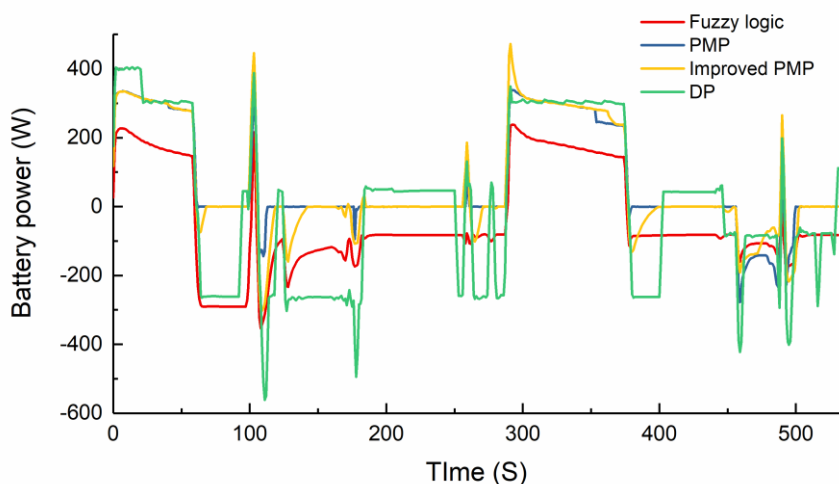**Figure 6.** Power spectrum of a fixed-wing UAV.

Figure 7. Fuel cell power.

Figure 8. Battery power.
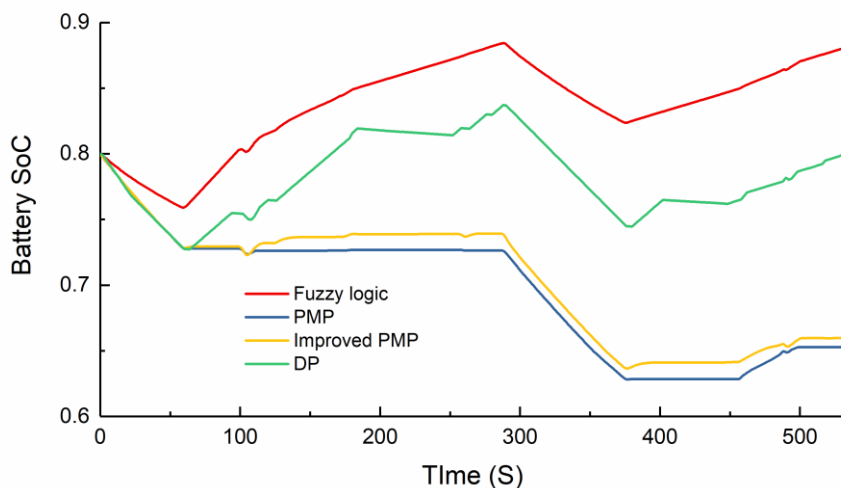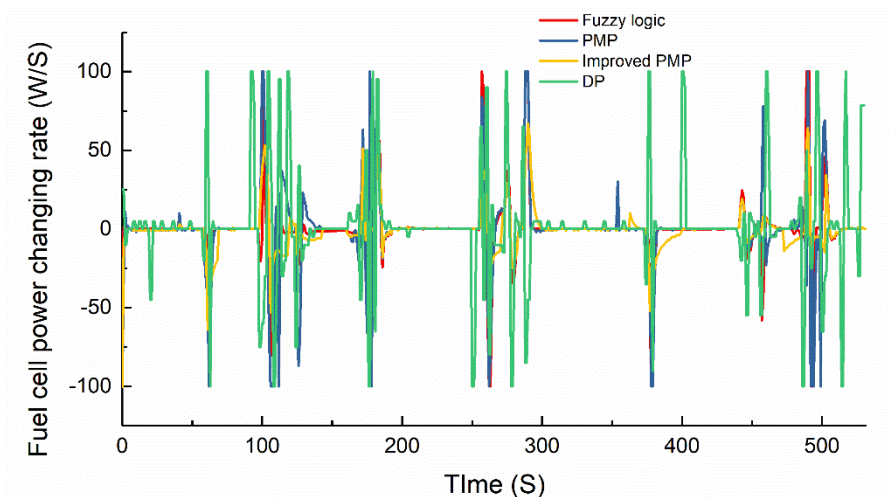

Figure 9. Battery SoC.

Figure 10. Fuel cell power changing rate.

Table 2. Equivalent hydrogen consumption

EMS	Equivalent hydrogen consumption (g)
Fuzzy logic	5.79
Basic PMP	5.46
Improved PMP	5.48
DP	5.72

Figure 7 show that the change of the fuel cell power under the fuzzy logic-based EMS is neither as drastic as that under the DP strategy nor as smooth as that under the PMP strategy. For example, for a sudden increase in the load power at approximately 260s, the change in the fuel cell output power based on the FL strategy was more obvious than that in the PMP. The fuel cell output power curves of the basic PMP and the improved PMP were the smoothest showing a more consistent trend, which was generally similar. This was because the fuel cell power changing rate was directly limited in the basic PMP, while the improved PMP further constrained the fuel cell power changing rate based on the basic PMP; hence, the fuel cell power of the improved PMP was smoother than that of the basic PMP. Unlike the two PMP-based EMS, DP achieved global optimization. However, the effect of regulating the working conditions of the fuel cell was not good, and the fuel cell output power under the DP strategy drastically fluctuated around 60 s, 120 s, 180 s, 260 s, 400 s, 460 s, and 520 s of the simulation analysis, while the fuel cell output power under the other three strategies was relatively flat. The fuel cell power changing rate data from Figure 10 also verified the above analysis.

Figure 8 depicts that the battery power and the change of the battery SoC reflects the change of the battery power. We focused herein on the changing characteristics of the battery SoC. Figure 9 shows that the battery SoC of the hybrid system remained around SOC_{ref}, which is not higher than the preset SOC_{max} or lower than SOC_{min} when based on the four different EMSs. The battery SoC variation under four different strategies was influenced by the load situation and had a relatively similar trend. The

battery SoC under all strategies showed a significant decrease within 0–60 s. In the subsequent time interval of 60–300 s, the battery SoC stopped decreasing and showed a relatively stable or rebounding trend. The battery SoC decreased again in the 300–380 s interval. The battery was then charged, and the SoC kept rising. Compared with the PMP, the battery SoC based on the fuzzy logic strategy had a non-significant decreasing trend in the time interval of 0–60 s and 300–380 s, but showed a more obvious increase in the time intervals of 60–300 s and 380–530 s. The SoC variation curves under the basic PMP and improved PMP strategies were close to each other, and overlapped almost completely in the first 60 s of the simulation. They were also very similar in the subsequent simulations. The SoC under the improved PMP was always slightly higher than that under the basic PMP. Both DP and PMP are global optimization-based energy management strategies, and the battery SoC based on DP has a very similar performance to PMP in the 0–60 s time interval. The battery SoC was always between FL and PMP. An additional point to note is that the battery SoC based on the DP strategy had the same value at the end of the simulation as at the beginning, while none of the other centralized strategies showed this feature.

Figure 10 shows the fuel cell power changing rate. The power changing rate of the fuel cell under the PMP strategy was relatively small, while the variation rate of the fuel cell under the DP strategy was relatively large. The fuel cell power changed most frequently under the DP strategy, probably because the DP algorithm cannot impose a constraint on the output power change rate of the fuel cell. In contrast, the fuel cell power variation rate was effectively controlled under the PMP strategy. The fuel cell output power variation rate based on the improved PMP was lower than that in the basic PMP because of the further constraint on the fuel cell output power variation rate imposed by the improved PMP based on the basic PMP.

The strategy proposed in this paper was more effective than the strategy proposed in the literature [15] in maintaining the battery SoC and avoiding the overload output of the fuel cell. Compared with the online fuzzy strategy in the literature [15] where the battery SoC decreases roughly by 0.25, the fuzzy logic strategy in this paper had more complex fuzzy rules and the degree of battery SoC fluctuation was less than 0.1, which can effectively avoid overcharging and discharging of the UAV battery under complex load conditions and was conducive to improving the battery durability, which was an outstanding advantage of the FL strategy. Compared to the passive and state machine strategies in [15], the three strategies proposed in this paper, DP, PMP, and improved PMP, were effective in avoiding the heavy load output of the fuel cell. The fuel cell operated at close to the rated power based on the passive and state machine strategies in [15], the strategy proposed in this paper gives the fuel cell the ability to operated at lower power while using the battery to absorb most of the power fluctuations. For example, based on the PMP strategy proposed in this paper, the fuel cell only operated at about half of the rated power at the 200s of the simulation, which had a positive impact on the protection of the fuel cell life. This is another advantage of the strategy proposed in this paper compared to other strategies.

Table 2 demonstrates the equivalent hydrogen consumption of the fuzzy logic, PMP, improved PMP, and DP as 5.79 g, 5.46 g, 5.48 g, and 5.72 g, respectively. The proposed improved PMP-based EMS can effectively save 5.4 % fuel compared with fuzzy logic. In short, the proposed improved PMP-based EMS excels fuzzy logic and DP, and approximate to the basic PMP. Thus, the proposed EMS demonstrates good cost economy and fuel cell power changing rate, confirming its superiority, which can be converted into an improvement in the fuel cell lifetime and durability.

5. CONCLUSIONS

This study investigated the EMS of a fixed-wing fuel cell hybrid-powered UAV. First, we analyzed the energy flows of a fixed-wing UAV powered by a hybrid system. Next, the system mathematical model of the hybrid UAV was developed. Three EMSs, namely fuzzy logic, DP, and PMP, were proposed for hybrid UAVs to achieve a reasonable power distribution among different power sources. The adverse effects of the output current and the power variation rate of the fuel cell on the lifetime were further considered based on the basic PMP. The simulation results obtained in the MATLAB environment using an actual load spectrum showed that fuzzy logic was robust and suitable for real-time control, albeit its hydrogen consumption. DP can be used as an offline evaluation criterion. PMP-based EMSs are effective in extending the endurance of the UAV while reducing the change rate of the fuel cell power and improving the adverse effects on the battery lifetime. The improved PMP has the smallest fuel cell power changing rate, saving 5.4 % hydrogen compared with fuzzy logic, which is a recommended EMS. The theory proposed herein can be generally applied to various hybrid systems, which is important for the practical development of UAVs. The fuel cell and battery durabilities in hybrid UAVs will be investigated in the future.

References

1. M. Hassanalian, A. Abdelkefi, *Progress in Aerospace Sciences*, 91 (2017) 99–131.
2. M. Jaeger, D. Adair, *Materials Today-Proceedings*, 4 (2017) 4458–4468.
3. M.N. Boukoberine, Z.B. Zhou, M. Benbouzid, *Applied Energy*, 255 (2019) 22.
4. H.S. Das, M.M. Rahman, S. Li, C.W. Tan, *Renewable & Sustainable Energy Reviews*, 120 (2020) 27.
5. A.M. Mazur, R. Domanski, *Aircraft Engineering and Aerospace Technology*, 91 (2019) 736–746.
6. Y. Zhou, A. Ravey, M.C. Pera, *Applied Energy*, 258 (2020) 17.
7. A. Gong, D. Verstraete, *International Journal of Hydrogen Energy*, 42 (2017) 21311–21333.
8. T. Lei, Z. Yang, Z. Lin, X. Zhang, *Chinese Journal of Aeronautics*, 32 (2019) 1488–1503.
9. B. Wang, D. Zhao, W.X. Li, Z.Y. Wang, Y. Huang, Y.C. You, S. Becker, *Progress in Aerospace Sciences*, 116 (2020) 22.
10. X.Q. Lu, Y.B. Wu, J. Lian, Y.Y. Zhang, C. Chen, P.S. Wang, L.Z. Meng, *Energy Conversion and Management*, 205 (2020) 26.
11. N. Sulaiman, M.A. Hannan, A. Mohamed, P.J. Ker, E.H. Majlan, W.R.W. Daud, *Applied Energy*, 228 (2018) 2061–2079.
12. C. Liu, Y.J. Wang, L. Wang, Z.H. Chen, *Journal of Power Sources*, 438 (2019) 13.
13. M.A. Khan, A. Khan, M. Ahmad, S. Saleem, M.S. Aziz, S. Hussain, F.M. Khan, *Arabian Journal for Science and Engineering*, 46 (2021) 1179–1198.
14. S. Al, Y. Xie, K. Malandrakis, M. Lopez, A. Tsourdos, Ieee, 2016 24th Mediterranean Conference on Control and Automation, (2016), pp. 1242–1247.

15. X.H. Zhang, L. Liu, Y.L. Dai, T.H. Lu, *International Journal of Hydrogen Energy*, 43 (2018) 10094–10103.
16. V. Larsson, L. Johannesson, B. Egardt, *Ieee Transactions on Vehicular Technology*, 64 (2015) 1458–1467.
17. K. Ou, W.-W. Yuan, M. Choi, S. Yang, S. Jung, Y.-B. Kim, *International Journal of Hydrogen Energy*, 43 (2018) 15433–15444.
18. S. Ahmadi, S.M.T. Bathaee, A.H. Hosseinpour, *Energy Conversion and Management*, 160 (2018) 74–84.
19. H. Li, A. Ravey, A. N'Diaye, A. Djerdir, *Journal of Power Sources*, 395 (2018) 262–270.
20. Y. Xie, A. Savvaris, A. Tsourdos, *Aerospace Science and Technology*, 85 (2019) 13–23.
21. T. Li, H. Liu, H. Wang, Y. Yao, *Ieee Access*, 8 (2020) 25927–25937.
22. S.B. Xie, X.S. Hu, Z.K. Xin, J. Brighton, *Applied Energy*, 236 (2019) 893–905.
23. H. Marzougui, A. Kadri, J.-P. Martin, M. Amari, S. Pierfederici, F. Bacha, *Energy Conversion and Management*, 195 (2019) 830–843.
24. A.M. Bassam, A.B. Phillips, S.R. Turnock, P.A. Wilson, *International Journal of Hydrogen Energy*, 42 (2017) 623–635.
25. X.H. Zhang, L. Liu, Y.L. Dai, *International Journal of Aerospace Engineering*, 2018 (2018) 16.
26. H. Rezk, A.M. Nassef, M.A. Abdelkareem, A.H. Alami, A. Fathy, *International Journal of Hydrogen Energy*, 46 (2021) 6110–6126.
27. K. Kaya, Y. Hames, Ieee, A Study on Fuel Cell Electric Unmanned Aerial Vehicle, Ieee, (2019) New York.
28. J. Jia, Q. Li, Y. Wang, Y.T. Cham, M. Han, *Ieee Transactions on Energy Conversion*, 24 (2009) 283–291.
29. P.R. Pathapati, X. Xue, J. Tang, *Renewable Energy*, 30 (2005) 1–22.
30. LEI，Tao, MIN，Zhihao, FU，Hongjie, ZHANG，Xingyu, LI，Weilin, ZHANG，Xiaobin, *Acta Aeronautica et Astronautica Sinica*, 41 (2020) 293–307